International Journal of Thermal Sciences 48 (2009) 2365–2374

Contents lists available at ScienceDirect

International Journal of Thermal Sciences

journal homepage: www.elsevier.com/locate/ijts

Computer simulation of ground-coupled liquid desiccant air conditioner for sub-tropical regions

C.K. Lee*, H.N. Lam

Department of Mechanical Engineering, University of Hong Kong, Pokfulam Road, Hong Kong

ARTICLE INFO

Article history:
Received 12 September 2008
Received in revised form
20 May 2009
Accepted 22 May 2009
Available online 24 June 2009

Keywords:
Ground-source heat pump
Ground heat exchanger
Borehole
Borefield
Liquid desiccant
Vapour compression cycle

ABSTRACT

Computer model for a novel ground-coupled liquid desiccant air conditioner (GCLDAC) was developed in which a liquid desiccant cycle selectively operated in parallel with a conventional ground-source heat pump cycle by employing just a single compressor. Reverse cycle operation was incorporated to provide heating in winter. Dynamic simulation was carried out for a single-zone sample building at two occupancy levels based on the weather data for Hong Kong and compared with those obtained using a conventional ground-source heat pump system (GSHP). It was found that the borehole length for GCLDAC was reduced by 10.1% on average under different groundwater velocities at a low occupancy level corresponding to a fresh air ratio of 0.066. A larger average reduction of 14.3% could be reached for a higher occupancy level corresponding to a fresh air ratio of 0.122. The energy consumptions for both systems were very close even when the additional parasitic energy consumption for GCLDAC was accounted for. A simple economic analysis indicated that if the borehole installation cost exceeded USD35.0/m, cost saving could be found for the new system at both occupancy levels. Should GCLDAC be manufactured in a low-cost region like China, the economic benefit could be furthered enhanced.

1. Introduction

Ground-source heat pump systems (GSHP), employing the ground as a media of heat exchange with the surrounding through vertical borehole ground heat exchangers, offer a higher energy efficiency than air-cooled systems and a consequent reduction in CO_2 emission. Also, the rejection of condensing heat to the ground helps relieve the heat island effect. However, drilling of deep boreholes involves a high initial cost, especially for sub-tropical regions with cooling-dominated loading profiles. To reduce cost, hybrid systems are developed. The most common design is the parallel operation of ground heat exchangers and cooling towers which is cost-effective. However, the use of fresh water cooling towers increases the risk of Legionnaires' disease. Moreover, fresh water can be a scarce resource nowadays in some regions and its adequate supply may be limited to certain periods of time. The use of sea water cooling towers depends on the availability of the sea water. If conventional air-cooled systems are used as the partner system, the overall system efficiency will be decreased. Hence, a new alternative is needed. The coupling with liquid desiccant dehumidification system offers a possibility.

Fig. 1 depicts the schematic diagram of a novel ground-coupled liquid desiccant air conditioner (GCLDAC) proposed for this application in cooling mode operation. A single compressor is used to provide desiccant cooling and heating in the liquid desiccant circuit for treating the fresh air and auxiliary cooling/heating to the supply air to meet the room loading requirement. The liquid desiccant circuit only operates in cooling mode through the use of two 3-way bypass valves to control a fixed proportion of the refrigerant flowing into the desiccant cooler/heater. The employment of a liquid desiccant system to handle fresh air only prevents a high regeneration temperature to be used for the liquid desiccant, thus maintaining the energy efficiency of the entire system. The annual unbalance of loading to the ground heat exchangers is reduced by transferring some of the condensing heat to the leaving regenerative air stream. The required borehole length can thus be shortened. Reverse cycle operation is achieved with the aid of two four-way selector valves for the refrigerant to provide heating in winter with all the refrigerant flowing through the supply air and ground-coupled coils only. In this study, dynamic simulation will be made to apply GLCDAC to a single-zone sample building based on the Hong Kong weather data from 1986 to 1995 at different groundwater flow velocities. Comparison with a conventional GSHP allows the potential reduction in borehole length to be estimated, and the corresponding impact on energy efficiency and cost analysed.

* Corresponding author.
E-mail address: a8304506@graduate.hku.hk (C.K. Lee).

1290-0729/$ – see front matter © 2009 Elsevier Masson SAS. All rights reserved.
doi:10.1016/j.ijthermalsci.2009.05.010

Nomenclature

a'	Specific interfacial surface area of packing ($m^2\,m^{-3}$)
C	Capacity rate according to Eq. (9) ($kW\,K^{-1}$)
c	Specific heat capacity ($kJ\,kg^{-1}\,K^{-1}$)
Cap	Heat capacity ($kJ\,K^{-1}$)
COP	Coefficient of performance
d_c	Packed column diameter (m)
d_p	Diameter of packing (m)
D_G	Diffusion coefficient of water ($m^2\,s^{-1}$)
F	Overall mass transfer coefficient ($kmol\,m^{-2}\,s^{-1}$)
G'	Superficial air mass flowrate ($kg\,m^{-2}\,s^{-1}$)
H	Enthalpy rate (kW)
h	Specific enthalpy ($kJ\,kg^{-1}$)
h'_c	Convective heat transfer coefficient corrected for simultaneous heat and mass transfer ($kW\,m^{-2}\,K^{-1}$)
h_d	Specific heat of dilution ($kJ\,kg^{-1}$)
k	Thermal conductivity ($W\,m^{-1}\,K^{-1}$)
L'	Superficial desiccant mass flowrate ($kg\,m^{-2}\,s^{-1}$)
m	Mass flowrate ($kg\,s^{-1}$)
M_w	Molecular weight of water ($kg\,kmol^{-1}$)
n_{ac}	Number of discretisation segments for air cooler
NTU	$=UA/C_{min}$ according to Eq. (9)
P	Pressure (kPa)
P_t	Liquid desiccant system pressure (kPa)
Pr	Prandtl number according to Eq. (7)
Q	Building load (kW)
Re	Reynolds number according to Eq. (7)
Sc	Schmidt number according to Eq. (7)
T	Temperature (°C or K)
t	Time (s)
UA	Overall heat transfer coefficient ($kW\,K^{-1}$)
V_G	Velocity of gas in packed column ($m\,s^{-1}$)
VOL	Volume (m^3)
W_{comp}	Compressor power input (kW)
x, y	Transverse directions of the ground surrounding the boreholes
x'	Portion of coil at different refrigerant regions
z	Vertical direction of the ground surrounding the boreholes
z'	Linear distance along tower height (m)

Greek symbols

β'	$=(T_r - T_{f,in})C_f/m_r\Delta h_{f'g'}$ according to Eq. (A4)
$\Delta h_{f'g'}$	Refrigerant specific enthalpy change across saturated region ($kJ\,kg^{-1}$)
$\Delta\rho_{f'g'}$	Refrigerant density change across saturated region ($kg\,m^{-3}$)
Δt	Discretisation time step (s)
ε	Heat transfer effectiveness
γ'	$=\rho_{g'}+\Delta\rho_{f'g'}(\chi_{in}+\beta' e^{-NTU})$ according to Eq. (A7) ($kg\,m^{-3}$)
λ	Specific latent heat of evaporation of water ($kJ\,kg^{-1}$)
ℓ	Characteristic length across coil
μ	Dynamic viscosity ($kg\,m^{-1}\,s^{-1}$)
ρ	Density ($kg\,m^{-3}$)
$\overline{\rho}$	Mean density ($kg\,m^{-3}$)
ω	Humidity ratio of moist air
ξ	Liquid desiccant concentration
χ	Quality of refrigerant

Subscripts

a	Air
ac	Air cooler
co	Condenser outlet
cond	Condenser
dhi	Desiccant heater inlet
dis	Compressor discharge
dsa	Dry supply air
dzone	Dry zone air
f	Fluid
f′	Saturated liquid refrigerant
G	Gas
g′	Saturated gaseous refrigerant
i, j, m	Discretisation step of the ground in x, y and z directions
in	Inlet
L	Liquid desiccant
lat	Latent
max	Maximum
min	Minimum
r	Refrigerant
old	Conditions at previous time step
rta	Return air
sa	Supply air
sat	Saturated region
sc	Sub-cooled region
sen	Sensible
sh	Superheated region
suc	Compressor suction
w	Water
zone	Building zone

2. Literature review

In cooling-dominated regions, the coupling of ground-source heat pump systems with cooling towers has been used to reduce the lengths of the boreholes and consequently the installation cost. Kavanaugh and Rafferty [1] outlined a design methodology of such system. Kavanaugh [2] further revised the method and discussed the various cost consideration and operation criteria for the system. Yavuzturk [3] studied the performance of hybrid geothermal heat pump systems coupled with cooling towers based on his short time-step model for the ground heat exchangers. Other partner systems may be used. Ramamoorthy et al. [4] analysed a hybrid system that used a cooling pond as the supplemental heat rejecter. Lau and Suen [5] described an installation in Hong Kong which was also equipped with aqua-therm heat exchangers for emergency backup. Gasparella et al. [6] reported the operation of a combined liquid desiccant and geothermal heat pump system in Italy with different operation modes in various seasons.

In heating-dominated regions, auxiliary heating source is needed to relieve the ground temperature drop surrounding the boreholes during the operation in winter. This can be accomplished through the coupling with a solar system. Surplus heat can be injected into the ground and stored during the summer time. Ozgener and Hepbasli [7] discussed the costing of a solar-assisted geothermal heat pump system. Chiasson and Yavuzturk [8] analysed the performance of geothermal heat pump systems coupled with solar thermal collectors, and commented that the drilling costs for the boreholes should exceed USD32.81/m in order that the hybrid systems became economically viable. Chiasson et al. [9] detailed a school retrofit project which converted the existing

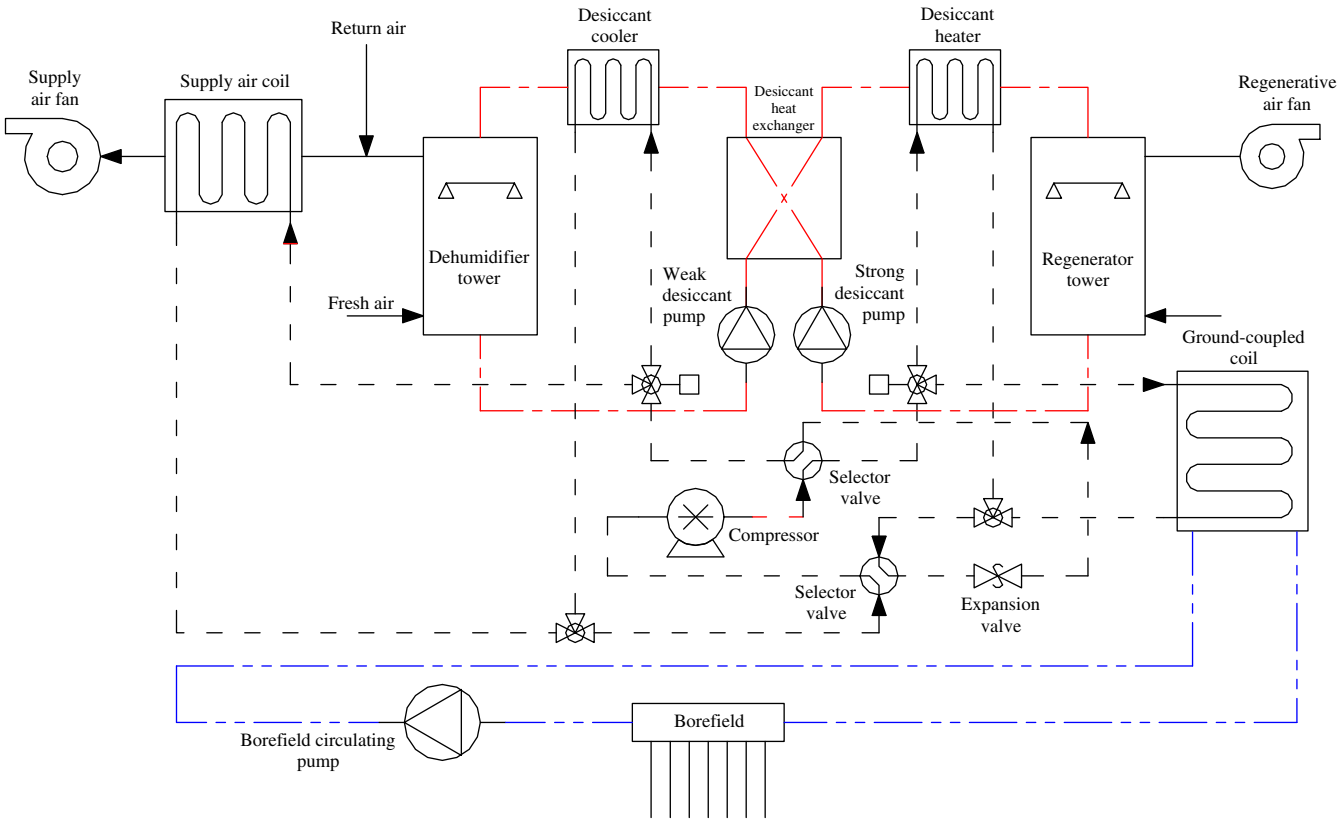

Fig. 1. Schematic diagram of a ground-coupled liquid desiccant air conditioner (GCLDAC).

conventional system to a solar-assisted geothermal heat pump system. Wu and Zheng [10] investigated a solar ground-source heat pump system coupled with PCM thermal storage to provide combined heating and cooling.

3. Mathematical formulation

3.1. Ground heat exchanger borefield

A three-dimensional implicit finite difference model employing rectangular coordinates system developed by Lee and Lam [11] will be used for the determination of the borefield performance. The entire ground volume is discretised and each borehole is represented by a square column with the square section circumscribed by the borehole radius, as shown in Fig. 2. The effect of groundwater is included by adding a convective term in the governing differential equation. The ground temperatures and fluid temperatures inside the boreholes will be solved simultaneously by using an iterative approach.

3.2. Liquid desiccant systems

In determining the conditions of the liquid desiccant around the cycle, the change of states across the pumps is assumed to be

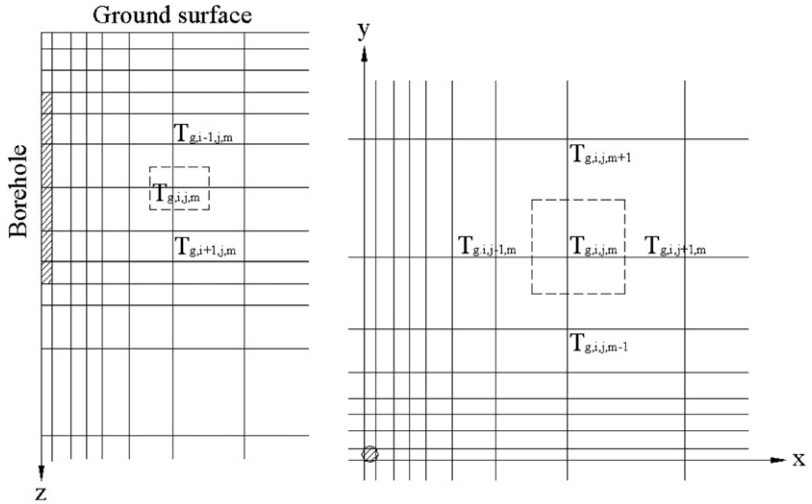

Fig. 2. Discretisation scheme for the ground surrounding a borehole.

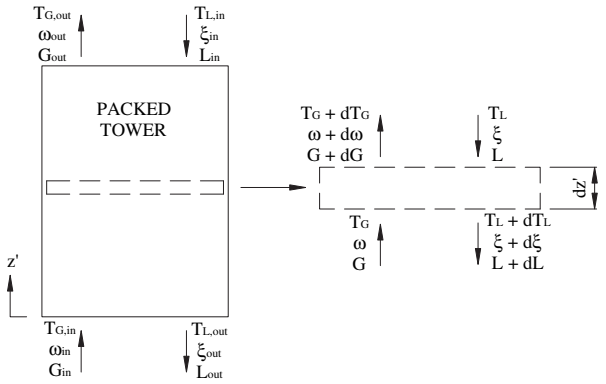

Fig. 3. Discretisation scheme of a packed tower.

negligible but the energy consumptions for the auxiliary pumps and fan will be accounted for and discussed in Section 5.

3.2.1. Desiccant packed tower

Fig. 3 indicates an elemental section of a vertical counter-flow liquid desiccant packed tower utilising lithium chloride solution as the liquid desiccant. According to Factor and Grossman [12], the moisture transfer rate between air and liquid desiccant depends on the corresponding partial pressures as

$$\frac{d\omega}{dz'} = \frac{M_w F_{wG} a'}{G'} \ln\left(\frac{1 - P_{wL}/P_t}{1 - P_{wG}/P_t}\right) \tag{1}$$

The sensible heat transfer between air and liquid desiccant is given as

$$\frac{dT_G}{dz'} = -\frac{h'_{c,G} a' (T_G - T_L)}{G' c_G} \tag{2}$$

$$-dH_G = G' c_G dT_G + dG' [c_w (T_G - T_L) + \lambda] \tag{3}$$

By balancing the energy change between the air and liquid desiccant,

$$dT_L = \frac{dH_G + h_d dL'}{L' c_L} \tag{4}$$

The water vapour pressure in, and specific enthalpy of dilution of the liquid desiccant solution can be calculated based on the empirical formulae proposed by Conde [13].

Chung et al. [14] proposed empirical correlations for determination of the heat and mass transfer coefficients for lithium chloride liquid desiccant packed tower as

$$F_{wG} a' \left(\frac{M_w d_p^2}{D_w \rho_w}\right) = 1.326 \times 10^{-4} (1 - \xi)^{-0.94} \left(\frac{L'}{G'}\right)^{0.27} \times Sc_G^{0.333} Re_G^{1.16} \tag{5}$$

$$h'_{c,G} a' \left(\frac{d_p^2}{k_G}\right) = 5.20 \times 10^{-5} (1 - \xi)^{1.56} \left(\frac{L'}{G'}\right)^{0.50} Pr_G^{0.333} Re_G^{1.6} \tag{6}$$

for random packing verified with experimental data for $103 < Re_G < 205$. Here,

$$Sc_G = \frac{\mu_G}{D_G \rho_G} \quad Re_G = \frac{d_c \rho_G V_G}{\mu_G} \quad Pr_G = \frac{c_G \mu_G}{k_G} \tag{7}$$

Table 1
Details of single-zone building for dynamic simulation.

Building size (m)	10(W) × 10(D) × 4(H)
Building thermal capacitance (kJ K^{-1})	4800
Lighting load (W m^{-2})	5
Internal gain, radiative (kW)	1
Internal gain, convective (kW)	1
Occupant activity	Seating, light work

The change of states along the entire tower will be solved simultaneously by using an iterative method for all segments along the tower.

3.2.2. Desiccant-to-desiccant heater exchanger

By adopting a constant or average overall heat transfer coefficient, the temperature effectiveness of a counter-flow fluid-to-fluid heater exchanger can be determined using the approach by Bejan [15] as

$$\varepsilon = \frac{1 - e^{[-NTU(1 - C_{min}/C_{max})]}}{1 - (C_{min}/C_{max}) e^{[-NTU(1 - C_{min}/C_{max})]}} \tag{8}$$

$$\text{where NTU} = \frac{UA}{C_{min}} \text{ and } C = mc \tag{9}$$

If $C_{min} \cong C_{max}$, Eq. (8) becomes

$$\varepsilon = \frac{NTU}{1 + NTU} \tag{10}$$

3.2.3. Desiccant heater/cooler

Detailed mathematical modelling will be carried out in subsequent sections to incorporate the performance of the condenser and evaporator of a heat pump.

3.3. Refrigerant systems

In this analysis, a thermostatic expansion valve is to be used for maintaining a constant degree of superheat at the compressor inlet. The approach based on energy, refrigerant flow and refrigerant charge balance as adopted by Domanski and Didion [16] will be used for cycle iteration. In calculating the refrigerant charge, only the condenser and evaporator and the liquid line will be considered. Pressure drops across the condenser, evaporator and all connecting pipelines are neglected.

3.3.1. Compressor

Being the most important component in a refrigerant circuit, the precision of the model for the compressor is very important. In view of this, empirical correlations for the refrigerant mass flowrate and compressor power provided by the compressor manufacturer (www.emersonclimate.com) will be used which are based on a specified degree of superheat equal to 5.56 °C at the compressor suction. The refrigerant discharge condition is determined from

$$W_{comp} = m_r (h_{r,dis} - h_{r,suc}) \tag{11}$$

3.3.2. Condenser or desiccant heater

In the condenser, the refrigerant can change from a superheated gas to a sub-cooled liquid if sufficient cooling is provided and the refrigerant leaves the condenser at least as a saturated mixture. However, there will be no change in the composition of the condensing fluid. Again, a constant or average overall heat transfer coefficient is adopted throughout the coil. To calculate the global

Table 2
Parameter values used for simulation of borehole performance.

Parameter	Value	Parameter	Value
Insulated depth of borehole below ground surface (m)	5	Effective ground thermal conductivity ($W\,m^{-1}\,K^{-1}$)	3.5
Number of tubes inside borehole	4	Effective ground thermal diffusivity ($m^2\,s^{-1}$)	1.62×10^{-6}
Borehole radius (m)	0.055	Fluid heat capacity ($J\,kg^{-1}\,K^{-1}$)	4190
U-tube outer radius (m)	0.016	Fluid density ($kg\,m^{-3}$)	1000
U-tube inner radius (m)	0.013	Fluid thermal conductivity ($W\,m^{-1}\,K^{-1}$)	0.614
Distance for tube centre from borehole centre (m)	0.03	Fluid dynamic viscosity ($kg\,m^{-1}\,s^{-1}$)	0.00086
Grout thermal conductivity ($W\,m^{-1}\,K^{-1}$)	1.3	Pipe thermal conductivity ($W\,m^{-1}\,K^{-1}$)	0.4

performance, the condenser coil is divided into three parts, namely superheated, saturated and sub-cooled stage. Here, x' $(0<x'<1)$ is the proportion of coil for each stage. Clearly,

$$x'_{\mathrm{cond,sc}}+x'_{\mathrm{cond,sat}}+x'_{\mathrm{cond,sh}}=1 \tag{12}$$

To further simplify the analysis, average specific heat capacities are used for the refrigerant along the superheated and sub-cooled regions.

In the superheated and sub-cooled stages, Eq. (8) is applicable. Since the mass flowrate and the specific heat capacity of the refrigerant is generally lower than that for the liquid desiccant,

$$\mathrm{NTU}_{\mathrm{cond,sh}}=\frac{x'_{\mathrm{cond,sh}}\mathrm{UA}_{\mathrm{cond}}}{C_{\mathrm{r,cond,sh}}}\ \text{and}\ \mathrm{NTU}_{\mathrm{cond,sc}}=\frac{x'_{\mathrm{cond,sc}}\mathrm{UA}_{\mathrm{cond}}}{C_{\mathrm{r,cond,sc}}} \tag{13}$$

In the saturated stage, the refrigerant temperature remains constant except for particular refrigerants such as R407C. The temperature effectiveness becomes

$$\varepsilon_{\mathrm{cond,sat}}=1-e^{-\mathrm{NTU}_{\mathrm{cond,sat}}}\ \text{and}\ \mathrm{NTU}_{\mathrm{cond,sh}}=\frac{x'_{\mathrm{cond,sat}}\mathrm{UA}_{\mathrm{cond}}}{C_{\mathrm{L,dhi}}} \tag{14}$$

The temperature of liquid desiccant and refrigerant at corresponding states are then calculated. The complete coil performance requires an iterative method with initial guesses for $x'_{\mathrm{cond,sh}}$, $x'_{\mathrm{cond,sat}}$ and $x'_{\mathrm{cond,sc}}$ respectively. With all parameters estimated, the refrigerant charge in the condenser can be calculated as

$$M_{\mathrm{r,cond}}=\mathrm{VOL}_{\mathrm{cond}}\left[x'_{\mathrm{cond,sat}}\overline{\rho}_{\mathrm{r,cond,sat}}+x'_{\mathrm{cond,sc}}\left(\frac{\rho_{\mathrm{r,cond,f'}}+\rho_{\mathrm{r,co}}}{2}\right)\right] \tag{15}$$

The derivation of $\overline{\rho}_{\mathrm{r,cond,sat}}$ is given in Appendix A.

3.3.3. Evaporator or desiccant cooler

The modelling of an evaporator is similar to that for a condenser except that no sub-cooling of refrigerant is considered and the refrigerant is assumed to enter the evaporator as a saturated mixture. The refrigerant may leave the evaporator as a superheated gas if it is sufficiently heated. All other assumptions remain the same unless the evaporating fluid is air, which will be dealt with in the next section. The derivations of the governing equations are similar to those for condensers.

3.3.4. Air cooler

The modelling of an air cooler is more complicated than the desiccant cooler due to the possibility of condensation for the air. Hence, the finite difference method is adopted. With the air cooler sub-divided into numerous segments (n_{ac}), the heat transfer rate across each segment is calculated from

$$\Delta H_{\mathrm{ac}}=\mathrm{UA}_{\mathrm{ac}}(T_{\mathrm{a}}-T_{\mathrm{r}})/n_{\mathrm{ac}} \tag{16}$$

The enthalpy changes in the air and refrigerant streams are given by

$$\Delta h_{\mathrm{a}}=-\Delta H_{\mathrm{ac}}/m_{\mathrm{a}}\ \text{and}\ \Delta h_{\mathrm{r}}=\Delta H_{\mathrm{ac}}/m_{\mathrm{r}} \tag{17}$$

The complete solution is obtained by writing Eqs. (16) and (17) consecutively for each coil segments and solving them iteratively. Different formulations will be used for the air enthalpy change in the dry and wet regions.

3.3.5. Single zone

To simplify the analysis, the zone material is assumed to be a lumped mass, and no time delay is considered in the response of the zone temperature and relative humidity to the corresponding heat load and supply air conditions. By balancing the energy and moisture across the zone at one time interval,

$$\begin{aligned}&Q_{\mathrm{sen}}=C_{\mathrm{sa}}(T_{\mathrm{rta}}-T_{\mathrm{sa}})+C_{\mathrm{zone}}(T_{\mathrm{rta}}-T_{\mathrm{zone,old}})C_{\mathrm{zone}}=\tfrac{Cap_{\mathrm{zone}}}{\Delta t}\\&T_{\mathrm{rta}}=\frac{Q_{\mathrm{sen}}+C_{\mathrm{sa}}T_{\mathrm{sa}}+C_{\mathrm{zone}}T_{\mathrm{zone,old}}}{C_{\mathrm{sa}}+C_{\mathrm{zone}}}\end{aligned} \tag{18}$$

$$\begin{aligned}\frac{Q_{\mathrm{lat}}}{\lambda}&=m_{\mathrm{dsa}}(\omega_{\mathrm{rta}}-\omega_{\mathrm{sa}})+\frac{M_{\mathrm{dzone}}(\omega_{rta}-\omega_{\mathrm{zone,old}})}{\Delta t}\\\omega_{\mathrm{rta}}&=\frac{\frac{Q_{\mathrm{lat}}}{\lambda}+m_{\mathrm{dsa}}\omega_{\mathrm{sa}}+\frac{M_{\mathrm{dzone}}\omega_{\mathrm{zone,old}}}{\Delta t}}{m_{\mathrm{dsa}}+\frac{M_{\mathrm{dzone}}}{\Delta t}}\end{aligned} \tag{19}$$

Table 3
Design requirement of GCLDAC/GSHP.

	Case 1	Case 2
Peak room sensible load (kW)	7.1	7.7
Peak room latent load (kW)	1.0	1.6
Supply air flow ($m^3\,s^{-1}$)	0.530	0.575
Supply air temperature (°C)	13.1	12.6
Fresh air amount ($m^3\,s^{-1}$)	0.035	0.070
Fresh air ratio	0.066	0.122
Unit design sensible load (kW)	7.6	9.0
Unit design latent load (kW)	2.3	4.2
Unit design total load (kW)	9.9	13.3

Table 4
Parameter values used for GSHP.

	Case 1	Case 2
Overall heat transfer value of supply air/ground-coupled coils ($kW\,K^{-1}$)	1.5	1.9
Volume of refrigerant in supply air coil (m^3)	0.006	0.008
Volume of refrigerant in ground-coupled coil (m^3)	0.006	0.008
Volume of refrigerant in liquid line (m^3)	0.0002	0.00025
Refrigerant charge (kg)	1.5	3.0
No. of discretisation segment for supply air coil	50	50
Borefield fluid mass flowrate ($kg\,s^{-1}$)	0.5	0.6
Compressor model used	ZH30K4E	ZH38K4E

Table 5
Parameter values used for GCLDAC.

	Case 1	Case 2
Overall heat transfer value ($kW\,K^{-1}$)		
Desiccant cooler	0.1	0.2
Desiccant heater	0.15	0.3
Supply air coil in cooling mode	1.3	1.7
Supply air coil in heating mode	1.5	1.9
Ground-coupled coil in cooling mode	1.3	1.7
Ground-coupled coil in heating mode	1.5	1.9
Desiccant heat exchanger	1.0	1.2
Volume of refrigerant in desiccant cooler/heater (m^3)	0.0005	0.0015
Volume of refrigerant in supply air/ground-coupled coil (m^3)	0.0055	0.0065
No. of discretisation segments for desiccant towers	50	50
Height of desiccant towers (m)	0.5	0.6
Cross-sectional area of dehumidifier tower (m^2)	0.0225	0.0625
Cross-sectional area of regenerator tower (m^2)	0.0625	0.1225
Packing size of dehumidifier/regenerator tower (m)	0.01	0.015
Regenerative air flow ($m^3\,s^{-1}$)	0.07	0.15
Liquid desiccant (LiCl) solution volume flowrate ($m^3\,s^{-1}$)	0.00004	0.00009
Ratio of refrigerant to desiccant cooler/heater	0.1	0.15

The return air conditions will become the "old" zone conditions in the next time step.

4. Methodologies for simulation and analysis

With the models for all the individual components derived in Section 3, dynamic simulation of the entire system is then made by using an iterative approach for each time step. The control mode is determined based on the zone temperature at the end of the previous time step. Then the performance of the GSHP/GCLDAC is calculated based on the prescribed return air/fresh air conditions, fluid temperature leaving the borefield and the control status. The resulting fluid temperature leaving the GSHP/GCLDAC is used to find a new borefield fluid leaving temperature through the ground heat exchanger model while the supply air conditions are used to determine the new zone/return air conditions through the zone model. Iteration is carried out until convergence is reached. The methodology to evaluate the performance of the GSHP has been mentioned in Section 3.3. Initial guessed values for the condensing and evaporating pressures are made and the state changes around the vapour compression cycle are calculated from the corresponding component models starting from the compressor. Newton's method is then employed to adjust the refrigerant pressures so that the degree of superheat at the compressor suction and the refrigerant charge in the system are equal to the preset values.

For the GCLDAC, the methodology is slightly more complicated due to the additional liquid desiccant circuit. To enhance the convergence of the iteration, the refrigerant circuit is consolidated into a single sub-system and the performance determined based on the approach for the GSHP. Initial guesses for the liquid desiccant temperatures entering the dehumidifier and regenerator towers as well as the liquid desiccant concentration entering the dehumidifier tower are made. The corresponding state changes across the components are then calculated in the sequence of the dehumidifier tower, the regenerator tower, the desiccant-to-desiccant heat exchanger and the refrigerant sub-system. Gauss–Seidal method with under-relaxation is used and the iteration is carried out until the states of the liquid desiccant entering the dehumidifier and regenerator towers converge.

Table 6
Performance of GSHP/GCLADC at design conditions.

	Case 1		Case 2	
	GSHP	GCLDAC	GSHP	GCLDAC
Supply air condition (°C)	12.8	12.9	12.6	12.6
Borehole fluid entering temperature (°C)	35.9	35.3	36.2	35.3
Cooling capacity (kW)	10.1	10.0	12.7	12.7
Load transferred to borehole (kW)	12.1	10.9	15.3	13.1
COP	4.97	4.94	5.11	5.15

Table 7
Simulation results of GSHP with borehole length 250 m at no groundwater flow for Case 1 within 1986–1995.

	After 1 year	After 10 years
Total cooling energy to room (kWh)	32,570	336,082
Total heating energy to borehole (kWh)	39,522	408,520
Total energy input to compressor (kWh)	6486	67,631
Maximum borehole fluid leaving temperature (°C)	30.5	31.7

Before starting the dynamic simulation, the system control method and operating mode have to be set first. A room thermostat with a dead band of 2 °C will be used to determine the cooling/heating mode of the system. The cooling setpoint is 24 °C and the heating setpoint is 20 °C. No humidity control will be made. The system is assumed to operate continuously. The borefield circulating pump is run when the system is operated in the cooling or heating mode. A simple single-zone building will be used for analysis, with details shown in Table 1. Two cases will be considered, the first one with ten occupants and second case with twenty occupants, which allows the effect of fresh air ratio to be investigated. No infiltration will be considered in the building. The TRNSYS software package will be used to generate a room loading profile for simulation. The design outdoor condition is 31 °C/83%RH which is the one with the largest humidity ratio (and hence water vapour pressure in the air) from 1986 to 1995. The design indoor condition is 24 °C/54%RH. Random packing will be assumed. Scroll compressor and R134a refrigerant will be used in the analysis.

A single borehole will be adopted in order to neglect the effect of groundwater direction as highlighted by Lee and Lam [17]. To increase the capacity of the borehole, double U-tubes with connection configuration 1–3,2–4 as recommended by Zeng et al. [18] will be selected, and the other borehole parameters are shown in Table 2. To develop an equal basis for the comparison between GCLDAC and GSHP, similar coil and refrigerant parameters will be used in both systems and other parameters selected so that the capacity of both systems will be almost the same. The same compressor model will be used. The corresponding borehole length based on same maximum borehole fluid leaving temperature within the simulated time period and the compressor power input (including the power consumed by the additional pumps and fan in

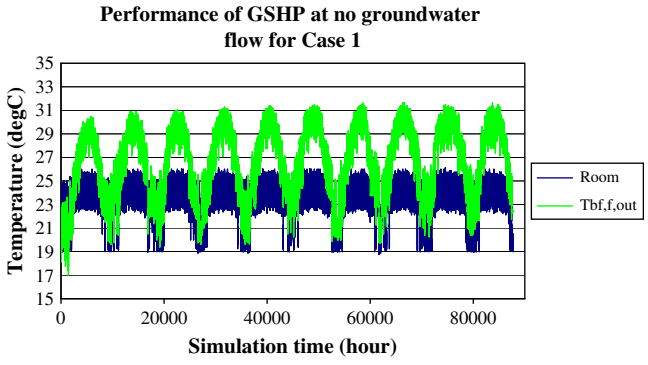

Fig. 4. Performance of GSHP at no groundwater flow for Case 1 for ten years.

Table 8
Simulation results of GCLDAC with borehole length 225 m at no groundwater flow for Case 1 within 1986–1995.

	After 1 year	After 10 years
Total cooling energy to room (kWh)	32,478	335,036
Total heating energy to borehole (kWh)	35,496	365,927
Total energy input to compressor (kWh)	6522	67,989
Maximum borehole fluid leaving temperature (°C)	30.5	31.7

the case of GCLDAC) will be investigated. Finally, a simple economic analysis will be made to justify the benefit of the new hybrid system for application in sub-tropical regions.

5. Results and discussions

5.1. Determination of design duty of GCLDAC/GSHP

Before the design parameters for the GSHP & GCLDAC could be set, the loading requirement had to be estimated first. The room loading demand generated using TRNSYS was used to determine the supply air condition which was assumed to be saturated moist air neglecting reheat through the process air fan and air duct corresponding to the design indoor condition of 24 °C and 54%RH. The peak sensible and latent loads were used for this purpose as only one supply air temperature could meet exactly the required sensible to latent load ratio. The fresh air requirement was calculated based on ASHRAE [19]. The loading requirement for the unit was then evaluated by adding the room loading to the ventilation load due to fresh air based on design outdoor condition of 31 °C and 83%RH as shown in Table 3.

5.2. Setting of design parameters of GCLDAC/GSHP

The next step involved the selection of the various coil, tower and refrigerant properties. In order to allow the possibility of reverse cycle operation, the volume and overall heat transfer values of the condenser and evaporator were chosen to be the same. For GCLDAC under the cooling mode, the condenser was composed of two coils, namely the ground-coupled coil and desiccant heater while the evaporator consisted of the supply air coil and desiccant cooler. The overall heat transfer values of coils reflected the mean temperature difference between the two fluids, and were selected so as to compromise between energy efficiency and equipment cost. In this analysis, the values were chosen so that the mean temperature difference would be between 5 and 10 °C. The parameters for the desiccant cycle were selected so that the loading of the two systems would be similar under comparable coil properties and with the same refrigerant charge. Tables 4 and 5 summarised the corresponding parameter values for GSHP and GCLDAC.

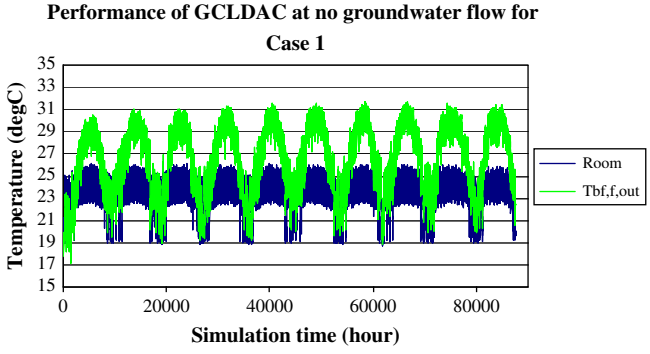

Fig. 5. Performance of GCLDAC at no groundwater flow for Case 1 for ten years.

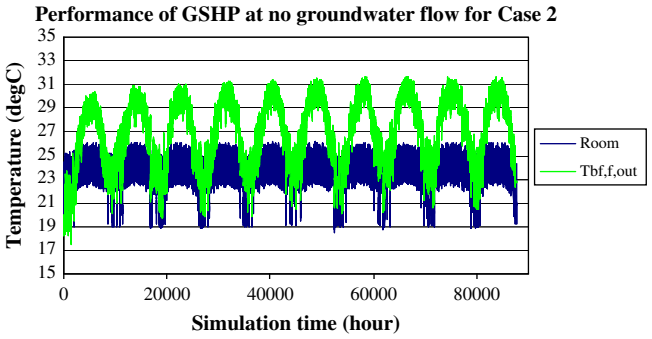

Fig. 6. Performance of GSHP at no groundwater flow for Case 2 for ten years.

5.3. Performance of GCLDAC/GSHP under design conditions

With the design parameters fixed, the performance of GCLDAC/GSHP under the design indoor/outdoor conditions was simulated and compared, with the results shown in Table 6. The borehole leaving fluid temperature was assumed to be 30 °C. The capacities of both systems were very close, but the load transferred to the borehole using GCLDAC was smaller. A 9% reduction was achieved for Case 1 while there was a 14.5% reduction for Case 2 in which the fresh air ratio was higher. The potential of the new hybrid system was thus clearly indicated. However, the system performance depended on the operation conditions, and an annual dynamic simulation was thus needed for an overall evaluation of the two systems for long-term use.

5.4. Dynamic simulation of GCLDAC/GSHP at no groundwater flow

To avoid too long a computation time, the simulation time step for the dynamic simulation was taken to be 15 min. The undisturbed ground temperature was assumed to be 20 °C. The first trial was made for Case 1 using GSHP with a borehole length of 250 m at no groundwater flow, and the results were shown in Table 7. The total energy transferred after the first year was smaller than the average value over the entire ten-year period. Based on the results from the first trial, the borehole length would be chosen to have the maximum borehole fluid leaving temperature maintained at around 31.7 °C after ten years-simulation in all ongoing simulations. Fig. 4 depicted the corresponding temperature profiles for the zone and fluid temperature leaving the boreholes.

Table 8 and Fig. 5 summarised the corresponding results using GCLDAC for Case 1 with a borehole length of 225 m upon repeated trials in order to maintain the same maximum borehole fluid leaving temperature. The total cooling energy to room was around 0.3% lower than that using GSHP after one year and ten years, while the estimation based on design conditions as shown in Table 6 indicated a reduction of less than 0.1%. The derivation was due to the fact that the performance of the two systems differed more at non-design conditions. The resulting zone conditions throughout the entire simulation period would not be exactly the same, and the energy transferred to the exhaust air would be different. The potential saving in borehole length for GCLDAC was 10%. The total energy transferred to borehole was 10.2% and 10.4% less than that with GSHP after one year and ten years respectively.

The total energy input to the compressor was only 0.5% higher for GCLDAC which was comparable to around 0.6% difference in COP based on the design conditions as shown in Table 6. The said

Table 9
Simulation results of GSHP/GCLDAC at no groundwater flow for Case 2.

	GSHP for 1986	GSHP for 1986–1995	GCLDAC for 1986
Total cooling energy to room (kWh)	44,868	462,838	44,821
Total heating energy to borehole (kWh)	54,339	561,622	46,428
Total energy input (kWh)	8686	90,785	8639
Maximum borehole fluid leaving temperature (°C)	30.5	31.7	30.5
Borehole length (m)	325	325	280

difference was very small. To estimate the energy consumption from the auxiliary pumps and fan, it was assumed that the liquid desiccant pump head was 5 kPa and the regenerative air fan head was 100 Pa. With an assumed efficiency of 50% for the desiccant pumps and regenerative air fan, the total power consumption was then 15 W. The operating time for the liquid desiccant system for a ten-year operation was 33,882 h. Hence, the corresponding total energy consumption was 508 kWh. Meanwhile, account should also be made for the decrease in the borefield circulating pump energy consumption due to the shortening of the borehole by 25 m. Based on a reduction of pump head by 8.75 kPa and a pump efficiency of 75%, the power saving was 5.8 W. The total operating hour for the borefield circulating pump was 34,089 for a ten-year operation at both the cooling and heating modes. The corresponding energy saving was 198 kWh. Hence, the overall auxiliary energy requirement was 310 kWh, which was considered negligible as it accounted for less than 0.5% of that consumed by the compressor. Consequently, the new hybrid system was capable of maintaining the energy efficiency of GSHP.

By reviewing Tables 7 and 8, the maximum borehole fluid leaving temperatures after one year were also very close for both systems, meaning that comparison of system performances could be made with one-year simulation only. This was definitely useful as the computation time for GCLDAC was extremely long due to the slow convergence in the desiccant loop. It took more than 9 days to perform the dynamic simulation for ten years using GCLDAC for Case 1, while less than 10 h was required with GSHP. Hence, in subsequent analysis, ten-year simulations would be made for GSHP under different situations for determining the borehole length, and the corresponding study for GCLDAC carried out with one-year simulations based on the same maximum borehole leaving fluid temperature after one year for GSHP.

Table 9 and Fig. 6 summarised the simulation results for Case 2. The situation was very similar to that for Case 1. The reduction in borehole length was 13.8% while the total heat energy to borehole was 14.6% lower for GCLDAC. The total energy input to compressor was 0.5% lower for GCLDAC, indicating that GCLDAC was slightly more energy-efficient, which was in line with the higher COP for GCLDAC at the design condition listed in Table 6. Clearly, the reduction in borehole length with the new hybrid system increased with the fresh air ratio. It could be expected that up to 20% saving in borehole length could be reached with a fresh air ratio of 0.15 which was common for applications with higher occupant density and/or indoor air quality requirement like schools or hospitals. Most importantly, the energy efficiency of GSHP could still be maintained, which meant that GCLDAC would be a potential alternative system for installation in sub-tropical regions if a reduction in the installation cost could be found. The zone temperature profiles shown in Figs. 4–6 indicated that the units were suitably sized in both cases in order to meet the design loadings. The heating period was short in each year which was typical for sub-tropical area and appeared to be similar in both cases.

5.5. Economic consideration

A precise economical analysis was difficult to be made, as the additional fabrication cost by combining the liquid desiccant system into a conventional geothermal heat pump could vary widely depending on the manufacturers' material sources and their production management quality. Hence, the analysis would only be based on the additional cost for the liquid desiccant system as a stand-alone product. Lowenstein et al. [20] suggested an average cost of USD21.2 per l/s of the process air. Of course there would be an extra cost for the additional pipework and control. However, cost savings could be made by fabricating one piece of equipment instead of two and by decreasing the sizes for the supply air and ground-coupled coils due to the reduced coil load requirement.

Very limited data was available for the installation cost of the boreholes in Hong Kong. Indeed, it depended strongly on the geology of the site, which could be much higher for long boreholes installed in hard rock. The local labour rate and the choice of the U-tubes were also important factors. Based on the information from the only installation in Hong Kong [5], the average cost was around USD30.0/m for shallow boreholes with a single U-tube. Hence, the cost reductions were USD8.0 and −USD134.0 for Case 1 and Case 2 respectively. The economic benefit for GCLDAC was not significant, and cost increase was even found in Case 2. At present, no accounts were made for a higher installation cost for the boreholes with double U-tubes. These could improve the situation. If the borehole installation cost rose to USD35.0/m, cost saving could also be found for Case 2. Moreover, if the extra cost for the liquid desiccant system could be substantially reduced by manufacturing

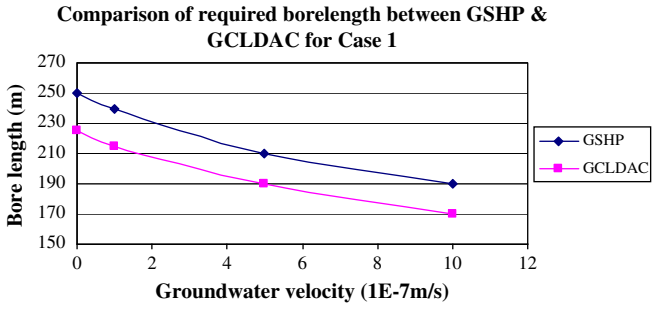

Fig. 7. Required borehole lengths of GSHP/GCLDAC at different groundwater velocities for Case 1.

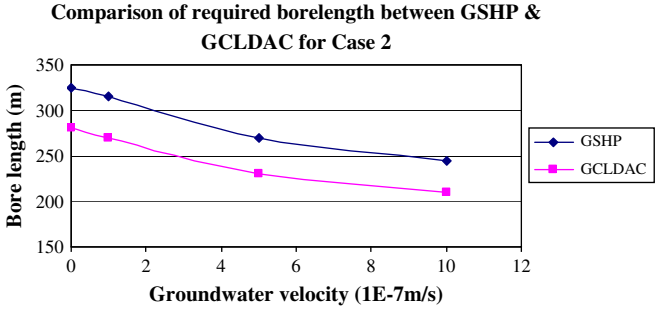

Fig. 8. Required borehole lengths of GSHP/GCLDAC at different groundwater velocities for Case 2.

the new hybrid system in a low-cost region like China, GDLDAC could become economically feasible, especially when applied in locations with a high installation cost for the boreholes. Indeed, if advances could be made in the liquid desiccant system design at limited extra production cost which allowed more condensing heat to be transferred to the regenerative air stream without deteriorating the energy efficiency of the hybrid system, the economic benefit of GDLADC could be further enhanced.

5.6. Dynamic simulation of GCLDAC/GSHP with groundwater flow

Performance of GCLDAC/GSHP was simulated using groundwater velocities of 10^{-7}, 5×10^{-7} and 10^{-6} m/s respectively for the two cases, and the corresponding required borehole lengths were shown in Figs. 7 and 8. The average reduction in borehole length for GCLDAC was 10.1% in Case 1 and 14.3% in Case 2 with very minor fluctuations at different groundwater velocities.

6. Conclusions

A new hybrid system, the ground-coupled liquid desiccant air conditioner, was designed where the fresh air was treated by the liquid desiccant cycle in cooling mode, and the mixed air handled by a conventional geothermal heat pump system. Only a single heat pump was needed to provide the necessary desiccant cooling/heating and air-conditioning load for the supply air. A single-zone sample building was used to analyse the dynamic performance of the new hybrid system. The room air-conditioning load profile was generated using the TRNSYS software package based on the Hong Kong weather data. Two cases were studied, the first one with 10 occupants corresponding to a fresh air ratio 0.066 and the second one with 20 occupants corresponding to a fresh air ratio 0.122. The simulated results were compared with those using only the conventional geothermal heat pump in terms of the required borehole length and total energy input to the compressor at different groundwater flow conditions.

With the new hybrid system, the borehole length was reduced by 10.1% on average for Case 1, while a 14.3% saving was achieved for Case 2, as part of condensing heat was transferred to the regenerative air stream of the liquid desiccant loop. Hence, for a design requiring a higher fresh air ratio as in Case 2, more beneficial results could be obtained. The total energy input to the compressor was nearly the same for both systems, and the energy consumption for the additional pumps and fan in GCLDAC accounted for less than 0.5% of that for the compressor. Hence, the new hybrid system did not cause deterioration in the energy efficiency of the conventional geothermal heat pump system. The groundwater flow did not affect the borehole length reduction significantly.

A simple economic analysis based on available cost data indicated that the economic benefit of GCLDAC in Case 1 was small, and cost increase was even found in Case 2. Indeed, the economic benefit of the new system depended on the cost level for borehole installation, which varied widely according to the different ground conditions and local labour rate. If the borehole installation cost exceeded USD35.0/m, cost saving could be achieved in both cases. The additional equipment cost could be reduced if manufactured in a low-cost region like China, which help to make the new system economically feasible.

Appendix A

Consider a counter-flow heat exchanger coil with heat transfer between a refrigerant and a fluid (air or any liquid). Assume that the refrigerant lies in the saturated region (constant temperature) throughout the entire coil and the heat capacity of the fluid remains constant. At some characteristic length ℓ ($0=$ fluid inlet, $1=$ refrigerant inlet),

$$C_f dT_f = UA\left(T_r - T_f\right)d\ell$$

$$dT_f = \frac{UA}{C_f}\left(T_r - T_f\right)d\ell$$

By setting $NTU = UA/C_f$ and re-arranging,

$$\frac{dT_f}{T_r - T_f} = NTU\,d\ell$$

Integrating and applying the boundary condition that at $\ell = 0$, $T_f = T_{f,in}$,

$$\ln\left(\frac{T_r - T_{f,in}}{T_r - T_f}\right) = NTU\cdot\ell$$

$$T_f = T_r - \left(T_r - T_{f,in}\right)e^{-NTU\cdot\ell} \tag{A1}$$

By equating the energy change between refrigerant and fluid,

$$C_f dT_f = m_r dh_r = -m_r \Delta h_{f'g'} d\chi$$

$$dT_f = -\frac{m_r \Delta h_{f'g'}}{C_f} d\chi \tag{A2}$$

where χ is the quality of the refrigerant. Combining Eqs. (A1) and (A2),

$$-\frac{m_r \Delta h_{f'g'}}{C_f} d\chi = NTU\left(T_r - T_{f,in}\right)e^{-NTU\cdot\ell} d\ell$$

$$d\chi = -\frac{NTU\left(T_r - T_{f,in}\right)C_f}{m_r \Delta h_{f'g'}} e^{-NTU\cdot\ell} d\ell$$

Integrating and setting $\chi = \chi_{in}$ at $\ell = 1$ and re-arranging,

$$\chi = \chi_{in} + \beta'\left(e^{-NTU} - e^{-NTU\cdot\ell}\right) \tag{A3}$$

$$\text{where } \beta' = \frac{\left(T_r - T_{f,in}\right)C_f}{m_r \Delta h_{f'g'}} \tag{A4}$$

The density of refrigerant at the saturated region is defined as

$$\rho_r = \frac{1}{\dfrac{\chi}{\rho_{g'}} + \dfrac{1-\chi}{\rho_{f'}}} = \frac{\rho_{g'}\rho_{f'}}{\rho_{g'} + \chi\Delta\rho_{f'g'}} \tag{A5}$$

where $\Delta\rho_{f'g'} = \rho_{f'} - \rho_{g'}$.

Substituting Eq. (A3) into Eq. (A5),

$$\rho_r = \frac{\rho_{g'}\rho_{f'}}{\rho_{g'} + \Delta\rho_{f'g'}\left[\chi_{in} + \beta'\left(e^{-NTU} - e^{-NTU\cdot\ell}\right)\right]} = \frac{\rho_{g'}\rho_{f'}}{\gamma' - \Delta\rho_{f'g'}\beta' e^{-NTU\cdot\ell}} \tag{A6}$$

$$\text{where } \gamma' = \rho_{g'} + \Delta\rho_{f'g'}\left(\chi_{in} + \beta' e^{-NTU}\right) \tag{A7}$$

The mean refrigerant density can be determined by integrating Eq. (A7) by dℓ from 0 to 1. Thus,

$$\begin{aligned}\overline{\rho}_{\mathrm{r}} &= \int_0^1 \rho_{\mathrm{r}}\mathrm{d}\ell = \int_0^1 \frac{\rho_{\mathrm{g}'}\rho_{\mathrm{f}'}}{\gamma' - \Delta\rho_{\mathrm{f}'\mathrm{g}'}\beta' e^{-\mathrm{NTU}\cdot L}}\mathrm{d}\ell \\ &= \rho_{\mathrm{g}'}\rho_{\mathrm{f}'}\left[\frac{\ell}{\gamma'} + \frac{1}{\gamma'\mathrm{NTU}}\ln\left(\gamma' - \Delta\rho_{\mathrm{f}'\mathrm{g}'}\beta' e^{-\mathrm{NTU}\cdot\ell}\right)\right]_0^1 \\ &= \rho_{\mathrm{g}'}\rho_{\mathrm{f}'}\left[\frac{1}{\gamma'} + \frac{1}{\gamma'\mathrm{NTU}}\ln\left(\frac{\gamma' - \Delta\rho_{\mathrm{f}'\mathrm{g}'}\beta' e^{-\mathrm{NTU}}}{\gamma' - \Delta\rho_{\mathrm{f}'\mathrm{g}'}\beta'}\right)\right] \end{aligned} \tag{A8}$$

References

[1] S.P. Kavanaugh, K. Rafferty, Ground-Source Heat Pumps: Design of Geothermal Systems for Commercial and Institutional Buildings, ASHRAE, Atlanta, 1997.

[2] S.P. Kavanaugh, A design method for hybrid ground-source heat pumps, ASHRAE Transactions 104 (2) (1998) 691–698.

[3] C. Yavuzturk, Modeling of Vertical Ground Loop Heat Exchangers for Ground Source Heat Pump Systems, Doctoral Thesis, Oklahoma State University, 1999.

[4] M. Ramamoorthy, H. Jin, A.D. Chiasson, A.D. Spitler, Optimal sizing of hybrid ground-source heat pump systems that use a cooling pond as a supplemental heat rejecter – a system simulation approach, ASHRAE Transactions 107 (1) (2001) 26–38.

[5] K.F. Lau, M.T. Suen, Geothermal heat pump air-conditioning system for the Hong Kong International Wetland Park, in: Proceedings of Shandong-Hong Kong Joint Symposium 2003, pp. A1–A9.

[6] A. Gasparella, G.A. Longo, R. Marra, Combination of ground source heat pumps with chemical dehumidification of air, Applied Thermal Engineering 25 (2–3) (2005) 295–308.

[7] O. Ozgener, A. Hepbasli, An economical analysis on a solar greenhouse integrated solar assisted geothermal heat pump system, Journal of Energy Resources Technology, Transactions of the ASME 128 (1) (2006) 28–34.

[8] A.D. Chiasson, C. Yavuzturk, Assessment of the viability of hybrid geothermal heat pump systems with solar thermal collectors, ASHRAE Transactions 109 (2) (2003) 487–500.

[9] A.D. Chiasson, C. Yavuzturk, W.J. Taibert, Design of school building HVAC retrofit with hybrid geothermal heat pump system, Journal of Architectural Engineering 10 (3) (2004) 103–111.

[10] L.X. Wu, M.Y. Zheng, Research of combined heating and cooling by solar ground-source heat pump and PCM thermal storage, in: Proceedings of the 2005 International Solar Energy Conference, 2005, pp. 379–394.

[11] C.K. Lee, H.N. Lam, Computer simulation of borehole ground heat exchangers for geothermal heat pump systems, Renewable Energy 33 (6) (2008) 1286–1296.

[12] H.M. Factor, G. Grossman, A packed bed dehumidifier/regenerator for solar air conditioning with liquid desiccants, Solar Energy 24 (6) (1980) 541–550.

[13] M.R. Conde, Properties of aqueous solutions of lithium and calcium chlorides: formulations for use in air conditioning equipment design, International Journal of Thermal Sciences 43 (4) (2004) 367–382.

[14] T.W. Chung, T.K. Ghosh, A.L. Hines, Comparison between random and structured packings for dehumidification of air by lithium chloride solutions in a packed column and their heat and mass transfer correlations, Industrial and Engineering Chemistry Research 35 (1) (1996) 192–198.

[15] A. Bejan, Heat Transfer, Wiley, 1993.

[16] P. Domanski, D. Didion, Mathematical model of an air-to-air heat pump equipped with a capillary tube, International Journal of Refrigeration 7 (4) (1984) 249–255.

[17] C.K. Lee, H.N. Lam, Effects of groundwater flow direction on performance of ground heat exchanger borefield in geothermal heat pump systems using 3-D finite difference method, in: Proceedings of Building Simulation 2007, Beijing, 2007, pp. 337–341.

[18] H. Zeng, N. Diao, Z. Fang, Heat transfer analysis of boreholes in vertical ground heat exchangers, International Journal of Heat and Mass Transfer 46 (23) (2003) 4467–4481.

[19] ASHRAE, Handbook: Fundamental, ASHRAE, Atlanta, 2005.

[20] A. Lowenstein, S. Slayzak, E. Kozubal, A zero carryover liquid-desiccant air conditioner for solar applications, in: Proceedings of ASME International Solar Energy Conference 2006, Denver, 2006, NREL/CP-550–39798.